Effect of morphology and support of copper nanoparticles on basic ovarian granulosa cell functions

Short title/running head: Copper nanoparticles effect on ovarian granulosa cells

Alexander V. Sirotkin[1*], Monika Radosová[1], Adam Tarko[1], Iris Martín-García[2], Francisco Alonso[2*]

[1] Constantine the Philosopher University in Nitra, Tr. A. Hlinku 1, 949 74 Nitra, Slovakia

[2] Instituto de Síntesis Orgánica (ISO) and Departamento de Química Orgánica, Facultad de Ciencias, Universidad de Alicante, Apdo. 99, 03080 Alicante, Spain

[*] Corresponding authors:

Prof. Dr. Alexander V. Sirotkin, PhD., DrSc., Constantine the Philosopher University, Tr. A Hlinku 1, 949 74 Nitra, Slovakia. E-mail: asirotkin@ukf.sk

Prof. Dr. Francisco Alonso, PhD., Instituto de Síntesis Orgánica (ISO) and Departamento de Química Orgánica, Facultad de Ciencias, Universidad de Alicante, Apdo. 99, 03080 Alicante, Spain. Email: falonso@ua.es

ABSTRACT

The aim of this survey is to explore the possible effects of unsupported (CuNPs) and supported copper nanoparticles (CuNPs/support) of different morphologies on basic ovarian

cell functions. For this purpose, we have compared the activity of unsupported spherical, triangular and hexagonal CuNPs, as well as of spherical CuNPs supported on titania, zeolite Y and activated charcoal (0, 1, 10 or 100 ng/mL) on cultured porcine ovarian granulosa cells. Cell viability, proliferation (accumulation of proliferating cell nuclear antigen, PCNA), apoptosis (accumulation of Bcl-2-associated X protein, bax) and release of steroid hormones progesterone, testosterone and 17β-estradiol have been analyzed by the Trypan blue test, quantitative immunocytochemistry and ELISA, respectively. Cell viability decreased after treatment with hexagonal CuNPs, whilst all the other CuNPs increased it. Unsupported spherical and hexagonal CuNPs, and spherical CuNPs/titania reduced PCNA accumulation; in contrast, an increase was noted for unsupported triangular CuNPs and CuNPs/zeolite Y. Bax accumulation was not affected by hexagonal CuNPs, whereas CuNPs/zeolite Y promoted it and all the other CuNPs depleted it. The release of all steroid hormones was inhibited by CuNPs/TiO_2 and stimulated by CuNPs/charcoal, whilst CuNPs/zeolite Y promoted the testosterone and 17β-estradiol output, but not that of progesterone.

These results demonstrate the direct, mainly stimulatory, impact of CuNPs on basic ovarian cell functions. The character of the CuNPs' action depends on their shape and support. Therefore, CuNPs with appropriate chemical modification could be potentially useful for the control of reproductive processes and treatment of reproductive disorders.

Key words: copper, nanoparticles, ovary, proliferation, apoptosis, hormones

1. INTRODUCTION

In the recent past, nanotechnology and the application of nano-metals (metal particles less than 100 nm size) have experienced a high growth rate (Kumar, 2009; Reddy et al., 2012;

Stark et al., 2015, Bhagyaraj et al., 2018). Copper nanoparticles (CuNPs) have shown a lot of promise as drugs for the treatment of osteoporosis, antibacterial and antifungal agents, contraceptives, in cancer imaging and therapy, and as farm animal food additives (Zhou et al., 2016; Rathore et al, 2018; Verma et al., 2019). They are used as fluorescent gas sensors, drug carriers, additives in lubricants, coatings for plastics, in catalysis and in other modern technologies (Gawande et al., 2016). Nevertheless, their application can be hampered by their toxicity for various living organisms (Hejazy et al., 2018; Ameh et al., 2019). For instance, it has been reported that CuNPs are toxic to fish, in some cases with comparable adverse effects to those of dissolved copper (Shaw et al., 2012; Al-Bairuty et al., 2013; Hedayati et al. 2016; Hoseini et al., 2016). Copper is a necessary co-factor for of a wide array of metabolic enzymes related to immune reactions, metabolism of neuromodulators, proteins and lipids (Pohanka, 2018). On the other hand, the adverse consequences of CuNPs on liver, spleen, kidney, respiratory system, neurons and DNA, which can induce cancer, have been well documented (Hejazy et al., 2018; Pohanka, 2019). The cyto- and genotoxic properties of CuNPs are mainly explained by their ability to produce reactive oxygen species, which induce both nuclear and cytoplasmic apoptosis (Roychoudhury et al., 2016; Hou et al., 2017; Ameh et al., 2019; Pohanka, 2019). In addition, the toxic impact of CuNPs can be due to their capacity to damage nuclear membranes, to act upon Ca^{2+} channels, nuclear factor kappa-light-chain-enhancer of activated B cells (NFkB) inflammatory transcription factor and mitogen-activated protein kinase which, in turn, are involved in DNA synthesis and damage (Hou et al., 2017).

The available data concerning copper and CuNPs' action on reproduction remain insufficient and contradictory. A body of evidence obtained on rodents demonstrated the capability of both copper and CuNPs to reduce gonadotropin and blood gonadal steroid hormones levels, to induce degenerative changes in gonads, ovarian follicular atresia, and to suppress gamete and

embryogenesis (Roychoudhury et al., 2016; Yang et al., 2017; Zhang et al., 2018). These adverse results could be related to the facility of CuNPs to suppress anti-oxidative enzymes and to induce ovarian cell apoptosis (Yang et al., 2017). Other studies, however, did not find any adverse effect of CuNPs on the number of mice ovarian follicles (Roychoudhury et al., 2016) and pregnancy (Zhang et al., 2018). Finally, some experiments revealed a stimulatory role of copper on porcine pituitary gonadotropin secretion (Roychoudhury et al., 2016), ovulation rate (Fevold et al., 1936), release of insulin-like growth factor I (IGF-I) and progesterone, and accumulation of both proliferation and suppressed apoptosis in cultured granulosa cells (Roychoudhury et al., 2014, 2016). Therefore, the available literature illustrates either positive or adverse behavior of copper or CuNPs on reproduction. This behavior could be mediated by pituitary gonadotropins, ovarian steroid hormones, and IGF-I and regulators/markers of both ovarian cell proliferation and apoptosis. Nonetheless, the reports concerning the characteristics of this activity on ovarian cells remain contradictory, and its elucidation and factors defining the type of the CuNPs' performance on the ovary require further studies.

The application of CuNPs and the production of safe CuNPs require understanding the factors influencing their outcome on physiological processes, including reproduction. The morphology of CuNPs, size, crystallinity, aggregation, surface properties and interaction with inorganic or organic supports can alter their catalytic properties (Gawande et al., 2016; Deka et al., 2019) and toxicity (Hou et al., 2017; Ameh et al., 2019). However, the influence of CuNPs' morphology and surface modification by association with other molecules on reproductive processes has not been studied yet.

Due to our ongoing interest on transition-metal nanoparticles (Alonso et al., 2008), we have studied the catalytic activity of both unsupported (Abdulkin et al., 2013) and supported CuNPs on different inorganic supports, such as activated charcoal (Mitrofanov et al., 2017),

zeolite Y (Alonso et al., 2015) and titania (Martín-García et al, 2018). We want to present herein a study to unveil (1) whether CuNPs can or cannot directly affect basic ovarian cell functions, (2) any possible effect of the morphology on the CuNPs' performance, and (3) the impact of the support on the CuNPs' activity. For this purpose, we have compared the influence of CuNPs of similar size but different shape (spherical, triangular, hexagonal) and that of spherical CuNPs supported on titania (CuNPs/TiO_2), zeolite Y (CuNPs/ZY) and activated charcoal (CuNPs/C) on the viability, proliferation, apoptosis and release of progesterone, testosterone and 17β-estradiol by cultured porcine ovarian granulosa cells. We have compared the dose-dependent action of these six types of CuNPs on cell viability, the accumulation of Bcl-2-associated X protein (bax, a marker of cytoplasmic apoptosis) (Peña-Blanco and García-Sáez, 2017), accumulation of proliferating cell nuclear antigen (PCNA, a proliferation marker) (Wang, 2014). In addition, we examined the influence of the CuNPs support on the secretory activity of ovarian cells. For this purpose, we analyzed the influence of CuNPs/TiO_2, CuNPs/ZY and CuNPs/C, added at different doses, on the release of the steroid hormones progesterone, testosterone and 17β-estradiol, the markers and regulators of ovarian cell functions (Sirotkin, 2014). Such a study has not been performed previously. It could be important for understanding the character and mechanisms of CuNPs' action, to search for factors affecting the biological activity of CuNPs, as well as to search for CuNPs that are suitable for therapeutic applications with minimal toxic side-effects.

2. MATERIALS AND METHODS

See the supporting information for general experimental information and nanoparticle characterization. The size of the CuNPs is expressed as the median ± standard deviation.

Preparation of unsupported copper nanoparticles

The syntheses of triangular and hexagonal CuNPs were carried out following the general procedure described by Carpenter's group (Carrol et al., 2011). This procedure involves the preparation of a 0.1 M solution of copper(II) chloride ($CuCl_2$) in the corresponding polyol (propylene glycol for triangular and diethylene glycol for hexagonal CuNPs), followed by the addition of NaOH (0.3 M) and reflux for 2 h. The resulting suspension was diluted with water at 50%. The obtained monodispersed CuNPs showed an average size of 1.27±0.37 and 1.81±0.52 nm for triangular (Fig. 1A) and hexagonal CuNPs (Fig. 1B), respectively.

Spherical CuNPs were prepared following the methodology of Alonso's group (Alonso et al., 2008). In a typical procedure, anhydrous $CuCl_2$ (97%, Aldrich; 134 mg, 1.0 mmol) was added to a suspension of lithium powder (Medalchemy S.L.; 14 mg, 2.0 mmol) and 4,4′-di-*tert*-butylbiphenyl (DTBB, Sigma-Aldrich; 27 mg, 0.1 mmol) in dry THF (20 mL) at room temperature under argon. The reaction mixture, which was initially dark green, changed to black, indicating that the suspension of CuNPs was formed. From this suspension, a 1.9 mL sample was diluted with deionized water (10 mL). Spherical CuNPs with an average size of 2.88±0.94 nm were obtained (Fig. 2).

Preparation of supported copper nanoparticles

The supported CuNPs were synthesized following the same methodology as above but, in this case, the black suspension was diluted with dry THF (18 mL) followed by the addition of the corresponding inorganic support (1.28 g): sodium Y zeolite (Sigma-Aldrich), activated charcoal (Norit CA1, Sigma-Aldrich) or TiO_2 (anatasa nanopowder, Alfa Aesar). Then, the resulting mixture was stirred for 1 h at room temperature, filtered, and the obtained solid was dried under air (TiO_2) or vacuum (zeolite Y and activated charcoal).

145 The materials showed monodispersed spherical CuNPs of average size 0.98±0.42 nm for TiO_2
146 (Mitrofanov et al., 2017) and 1.71±0.35 nm for zeolite Y (Alonso et al., 2015), and of
147 5.95±0.95 nm for activated charcoal (Alonso et al., 2011) (Fig. 2). The copper loading in
148 these materials was determined by inductively coupled plasma optical emission spectroscopy
149 (ICP-OES), being 1.9, 3.0 and 3.5 wt% for TiO_2, zeolite Y and activated charcoal,
150 respectively.

151 It must be mentioned that both the unsupported and supported CuNPs are obtained as a
152 mixture of Cu(I) and Cu(II) oxides due to exposure to air.

153 The characteristics of the unsupported and supported CuNPs and the methods used for their
154 characterization are described in the Supporting information file.

155 *Isolation and culture of granulosa cells*

156 Ovaries at the follicular phase of the ovarian cycle of non-cycling pubertal gilts,
157 approximately 180 days' age, were obtained after slaughter at a local slaughterhouse and
158 processed as described previously elsewhere (Roychoudhury et al., 2014; Sirotkin et al.,
159 2015). The collected granulosa cells at a final concentration of 10^6 cells/mL were cultured in
160 sterile DMEM/F12 1:1 medium supplemented with 10% fetal calf serum (both from
161 BioWhittakerTM, Verviers, Belgium) and 1% antibiotic-antimycotic solution (Sigma, St.
162 Louis, MO, USA) in 16-well (200 µL/well) chamber slides (Nunc Inc., International,
163 Naperville, USA). After 3–4 days' pre-culture, the medium (of the same composition as
164 above) was renewed, and the cells were cultured for 2 days in the medium with and without
165 the CuNPs listed above at the concentrations of 0, 1, 10 or 100 ng/mL. These are typical
166 CuNPs concentrations that have been tested in previous animal in-vivo and in-vitro
167 experiments (Liu et al., 2016; C A et al., 2018; Noureen et al., 2018; Sutunkova et al., 2018).
168 After two days of culture, the cells were washed with ice-cold PBS (pH 7.5), fixed in

paraformaldehyde (4% in PBS, pH 7.2–7.4; 60 min) and kept at 4 °C until immunocytochemical analysis. The culture medium was frozen at –17 °C to await RIA.

The nanoparticles were dispersed by gentle pipetting in the culture medium during 1 min, up to a concentration of 100 ng/mL, immediately before the addition to the cells.

Cell-viability test

Cell viability was evaluated by using the Trypan blue exclusion test, according to Strober (2001). Briefly, the medium from the culture plates was removed after incubation of the granulosa cells. Subsequently, the cell monolayer was subjected to Trypan blue staining (Sigma Aldrich, Hamburg, Germany) for 15 min. Following removal of this dye, the plates were washed twice with physiological solution and subjected to microscopic inspection (magnification: 400×). The ratio of dead (stained) cells to total cell count was calculated.

Immunocytochemical analysis of proliferation and apoptosis markers

The presence of PCNA and bax in the cells was detected by immunocytochemistry, as described previously elsewhere (Roychoudhury et al., 2014; Sirotkin et al., 2015), by using primary monoclonal antibodies against these molecules (all from Santa Cruz Biotechnology, Inc., Santa Cruz, USA). They were placed in either, a dilution of 1:500 in PBS secondary swine antibodies against mouse IgG labeled with horseradish peroxidase (Servac, Prague, Czech Republic, dilution of 1:1000) and visualized by staining with DAB-substrate (Roche Diagnostics GmbH, Manheim, Germany), or by secondary polyclonal goat antibodies against mouse IgGs labeled with the fluorescent marker fluorescein isothiocyanate (FITC; Santa Cruz Biotechnology, dilution 1:1000). The presence of molecules in the cells was determined using a light and fluorescence microscope (Leica GmbH, Wetzlar, Germany). Cells processed without the primary or secondary antibody were used as the negative controls. The cells expressing a signal greater than the background negative control levels were considered

positive. The proportion of cells containing visible molecules relative to the total cell number was calculated.

Immunoassay of hormones

Concentrations of progesterone, testosterone and 17β-estradiol were determined in 25 µL aliquots of incubation medium by the enzyme-linked immunosorbent assay (ELISA). Hormones were assayed using ELISA's kits according to the manufacturer's instructions (LDN Immunoassays and Services, Nodhorn, Germany).

Antiserum against progesterone cross-reacted ≤1.1% with 11-desoxycorticosterone, ≤0.35% with pregnenolone, ≤0.30% with 17α-hydroxyprogesterone, ≤0.20% with corticosterone, <0.10% with estriol, 17β-estradiol, testosterone, cortisone and 11-desoxycortisol, <0.02% with DHEA-S and cortisol. The sensitivity of the assay was 0.045 ng/mL. Intra- and inter-assay coefficients of variation did not exceed 5.40% and 5.59%, respectively.

The cross-reactivity of antiserum against testosterone was ≤3.3% with 11β-hydroxytestosterone and 19-nortestosterone, ≤0.9% with androstenedione, ≤0.8% with 5α-dihydrotestosterone, <0.1% with 17α-methyltestosterone, epitestosterone, E, P, cortisol, estrone and danazol. The maximal intra- and inter-assay coefficients of variation were 4.16% and 4.73%, respectively. Sensitivity of the assay was 0.083 ng/mL.

The sensitivity of the 17β-estradiol assay was 6.2 pg/mL. Intra- and inter-assay coefficients of variation did not exceed 6.4% and 4.5%, respectively. The cross-reactivity of antiserum against 17β-estradiol was ≤9.5% with fulvestrant, ≤4.2% with estrone, ≤3.8% with E2-3-glucuronide, ≤3.6% with E2-3-sulphate, ≤0.4% with estriol, <0.1% with androstenedione, 17α-hydroxyprogesterone, corticosterone, pregnenolone, E2-17-glucuronide, progesterone and testosterone.

All ELISA assays were validated for culture medium samples by dilution tests.

Statistical analysis

Each experiment was repeated three times using different animals (10–15 gilts per experiment). Each experimental group was represented by four chamber-slide wells. By RIA, blank control values were subtracted from the value determined in cell-conditioned serum-supplemented medium to exclude any non-specific background (less than 13% of the total values). Secretion rates were calculated per 10^6 cells/day or mg tissue/day. Differences between groups were evaluated using the Shapiro-Wilk's normality and Student's t-tests and Sigma Plot 11.0 (Systat Software, GmbH, Erkhart, Germany). Values are presented as the mean ± S.D. Differences were compared for statistical significance at P-levels less than 0.05 ($P < 0.05$).

3. RESULTS

The different types of nanoparticles tested in this study were prepared according to literature methods. In particular, spherical unsupported CuNPs (2.88±0.94 nm) were prepared by chemical reduction of copper(II) chloride with metal lithium as previously reported by us (Alonso et al., 2008), whereas triangular and hexagonal unsupported CuNPs were obtained by the polyol method following the general protocol by Carpenter's group (Carrol et al., 2011) (Fig. 1). It is noteworthy that the size of the triangular (1.27±0.37 nm) and hexagonal (1.81±0.52 nm) CuNPs decreased abruptly upon the addition of water, when compared with that observed by Carpenter's group for dried samples (*ca.* 50 nm) (Fig. 1). A common feature to all the unsupported CuNPs was their trend to grow by coalescence in the aqueous solution upon prolonged exposure to TEM irradiation. This behavior had a more pronounced effect in the triangular and hexagonal CuNPs, where the edges were rapidly blurred and the original

shape was more difficult to identify. Nevertheless, we have highlighted in Fig. 1B and 1C the shape of some of the mentioned CuNPs. The supported CuNPs were obtained by the aforementioned method of reduction of copper(II) chloride with metal lithium, followed by the addition of the inorganic support (titania, zeolite Y or activated charcoal) with stirring, filtration and drying. All supported CuNPs were spherical, being relatively small and monodispersed for those on titania (0.98±0.42 nm) and zeolite Y (1.71±0.35 nm), and larger for those on activated charcoal (5.95±0.95 nm) (Fig. 2). The CuNPs on titania (CuNPs/TiO_2, Fig. 2A) can be visually distinguished as very tiny spots on the larger but nanosized particles of the support (titania anatase nanopowder), whereas there is a sharp contrast between the CuNPs (foreground) and the zeolite Y support (background) (CuNPs/ZY, Fig. 2B). CuNPs are clearly observable as black spots on a grey charcoal background (CuNPs/C, Fig. 2C).

The comparison of spherical, triangular, hexagonal and spherical CuNPs/TiO_2, CuNPs/ZY and CuNPs/C showed substantial differences in their action on ovarian cell viability, proliferation, apoptosis and release of progesterone, testosterone and 17β-estradiol.

Both spherical (Fig. 3A) and triangular (Fig. 3B) CuNPs raised cell viability at all the doses added. On the contrary, hexagonal CuNPs decreased the viability of cells when added at doses of 10 and 100 ng/mL (Fig. 3C). Spherical CuNPs/TiO_2 (Fig. 3D), CuNPs/ZY (Fig. 3E) and CuNPs/C (Fig. 3F) triggered cell viability at doses of 10 and 100 ng/mL, 10 and 100 ng/mL and 100 ng/mL, respectively.

Spherical CuNPs lowered PCNA accumulation in the cells when added at doses of 1 or 10 ng/mL (Fig. 4A). Triangular CuNPs enhanced accumulation of this proliferation marker at all the doses added (Fig. 4B), whereas the hexagonal counterparts inhibited PCNA accumulation at all the doses added (Fig. 4C). CuNPs/TiO_2 reduced it at doses of 10 and 100 ng/mL (Fig. 4D), whilst CuNPs/ZY (Fig. 4E) and CuNPs/C (Fig. 4F) increased PCNA accumulation when added at all the doses or at 100 ng/mL, respectively.

Bax accumulation in the ovarian cells was suppressed by spherical CuNPs (at doses of 10 or 100 ng/mL, Fig. 5A) and triangular (at 100 ng/mL, Fig. 5B) but not by hexagonal ones (Fig. 5C). Spherical CuNPs/TiO_2 reduced bax accumulation at all the doses added (Fig. 5D). Conversely, when supported on zeolite Y, spherical CuNPs (at 1 or 10 ng/mL) resulted in significant promotion of bax accumulation (Fig. 5E). Bax accumulation fell at a dose of 100 ng/mL for CuNPs/C (Fig. 5F).

The analysis of progesterone release by cells cultured with CuNPs showed a drop in the progesterone output under the influence of CuNPs/TiO_2 (at all the doses added, Fig. 6A), but not under that of CuNPs/ZY (Fig. 6B). For CuNPs/C, as opposed to CuNPs/TiO_2, progesterone release was intensified at all the doses (Fig. 6C), whereas CuNPs/C at the highest dose (100 ng/mL) was less effective than at lower doses (1 or 10 ng/mL) (Fig. 6C).

T release was suppressed by CuNPs/TiO_2 (at all doses added) (Fig. 7A) but boosted by CuNPs/ZY (at 100 ng/mL, Fig. 7B) and CuNPs/C (at 10 and 100 ng/mL, Fig. 7C) in a dose-dependent manner.

Similar to the testosterone release, the 17β-estradiol output was reduced by CuNPs/TiO_2 (at 10 or 100 ng/mL, Fig. 8A) but rose by CuNPs/ZY (Fig. 8B) and CuNPs/C (Fig. 8C) at all the doses added. The effects of CuNPs/ZY and CuNPs/C on 17β-estradiol release have a dose-dependent character too.

DISCUSSION

The creation of a monolayer, high cell viability, presence of proliferation marker PCNA and production of steroid hormones indicate that the tested porcine granulosa cells were in good condition and suitable for analysis and testing of both the negative and positive behavior of CuNPs when given at physiological doses (Liu et al., 2016; C A et al., 2018; Noureen et al.,

2018; Sutunkova et al., 2018). Furthermore, the present observations demonstrate CuNPs directly affecting ovarian cells and their basic functions – viability, proliferation, apoptosis and release of hormones. These parameters are considered as both markers and regulators of ovarian functions and fecundity (Sirotkin, 2014). Additionally, the CuNPs' action on these parameters observed in our experiments, together with the previous reports (Fevold et al., 1936; Roychoudhury et al., 2014, 2016; Yang et al., 2017; Zhang et al., 2018), denote a CuNPs-triggered change on female reproductive functions, including fecundity. Moreover, they demonstrate that CuNPs can govern female reproductive processes, directly affecting various ovarian cell functions. Finally, comparison of the CuNPs performance on various read-outs points out the different role of CuNPs on female reproduction and their mechanisms. For example, they mean that most of the CuNPs tested in our experiments are not toxic. On the contrary, they can augment ovarian cell viability; only hexagonal CuNPs diminished it. Cell viability is defined by the balance between cell proliferation and apoptosis/death. The comparison of the CuNPs repercussion on PCNA and bax suggests that the gain of the cell viability under the CuNPs influence can be mainly due to suppression of cell apoptosis. In addition, triangular CuNPs and spherical CuNPs/C could raise cell viability also by promotion of cell proliferation. Finally, CuNPs/ZY could increment cell viability because they stimulated proliferation more than apoptosis. The adverse outcome for hexagonal CuNPs on cell viability can be explained by its ability to reduce cell proliferation without change in their apoptosis. On the other hand, we cannot exclude that cell viability can be defined not only by the PCNA/bax rate, but also by other regulators of cell proliferation and death (Pérez-Garijo and Steller, 2015; Fritsch et al., 2017; Gudipaty et al., 2018).

The CuNPs' action on cell proliferation and apoptosis can be mediated, in turn, by the role of CuNPs on the release of steroid hormones: the known auto-, para- and endocrine regulators of ovarian cell proliferation and apoptosis, ovarian follicullogenesis and resulted fecundity

(Sirotkin, 2014). The activity of supported CuNPs on three different supports was studied for progesterone, testosterone and 17β-estradiol release by ovarian cells. CuNPs/TiO_2 suppressed the release of these steroid hormones; opposite to this behavior, CuNPs/ZY and CuNPs/C mainly triggered the aforementioned release in a dose-dependent manner. The bell-shape effect of CuNPs/C on the progesterone output can be explained by the existence of adaptive negative feedback mechanisms preventing overstimulation of ovarian progesterone release, which could induce premature luteinization and suppression of ovarian follicullogenesis (Sirotkin, 2014). Both, stimulation and inhibition of the estrogen output can be explained by the corresponding changes in its precursors – testosterone and progesterone (Sirotkin, 2014). Further to this, 17β-estradiol is a known promoter of ovarian cell proliferation and inhibitor of cell apoptosis what, in turn, stimulates ovarian follicle growth and suppresses cell atresia (Sirotkin, 2014). Therefore, it is possible that the promotion of ovarian cell viability and proliferation by CuNPs/ZY, and the apoptosis inhibition by CuNPs/C could be explained by their capacity to foster ovarian steroidogenesis. The inhibition of cell proliferation and apoptosis, and the increase in cell viability by CuNPs/TiO_2 can be explained by the suppression of the steroid hormones release.

Our research is, probably, the first demonstration that the character of the CuNPs' action on reproductive functions can be defined by the morphology and support of the CuNPs. Understanding how the shape and support of CuNPs control their activity requires further studies. Nevertheless, it might be hypothesized that the CuNPs' properties can modify their capability to enter cellular membranes and affect the Ca^{2+} influx into the cells, intracellular protein kinases and transcription factors, metabolic and anti-oxidative enzymes, and the production of reactive oxygen species resulting in DNA damage (Hou et al., 2017; Yang et al., 2017; Pohanka, 2019). The differences in these characteristics could be possible causes of

inconsistency of the available reports concerning the type of consequences of CuNPs on the reproductive system and mentioned in the introduction.

Notwithstanding the limitation to rationalize the obtained results, it is worthwhile mentioning the distinctive behavior observed for hexagonal CuNPs: these nanoparticles are the only ones that reduce the ovarian cell viability and proliferation, inhibiting PCNA accumulation. It is known that the presence of vertices makes metal nanoparticles more reactive. Although this might be one reason of this particular behavior, the fact that the nanoparticles have been prepared in the presence of the somewhat toxic diethylene glycol must not be disregarded. As regards hormone release, the support seems to exert an outstanding role as only CuNPs/TiO_2 depletes or suppresses this function. Anatasa titania is composed of chains of distorted TiO_6 octahedra possessing undercoordinated atoms at the most abundant nanocrystal faces: i.e., 4- or 5-fold instead of 6-fold-coordinated Ti atoms, as well as 2-fold instead of 3-fold-coordinated O atoms (Bourikas et al., 2014); this makes titania particularly reactive. It is known that oxygen-containing molecules, such as water, can bind 5-fold-coordinated Ti atoms (through the water oxygen) and 2-fold-coordinated O atoms (through the water hydrogens). Therefore, an interaction of titania with the oxygen atoms of the three hormones or their precursors (more enhanced in the case of testosterone and 17β-estradiol because of the presence of hydroxyl groups in their structure) cannot be ruled out and might account for the particular effect observed for CuNPs/TiO_2 on hormone release.

From the practical viewpoint, the present investigation hints that several CuNPs cannot damage/suppress ovarian cell functions but even facilitate their viability, proliferation and secretory activity, suppressing their apoptosis. The lack of a visible toxic effect indicates the safety of their application, at least for reproductive health, although hexagonal CuNPs can be toxic (see below). Moreover, the potential utility of the stimulatory properties of CuNPs for the improvement of reproductive processes cannot be overruled. However, it must be taken

into account that the stimulatory properties of CuNPs resemble some signs of malignant transformation of ovarian cells, which are characterized just by these changes (Minorics and Zupko, 2018; Sharma et al., 2019). Therefore, the efficiency of CuNPs to induce such transformations should be carefully checked before application. On the other hand, the inhibitory action of hexagonal CuNPs on ovarian cell functions (reduction of cell viability and proliferation) illustrates a potential adverse consequence on female reproduction, as well as a potential usefulness for inhibition of reproductive processes or ovarian cancer. These indications should be, however, examined through both animal and human in-vivo experiments, including careful examination of possible toxic and stimulatory effects of CuNPs, given at the appropriate doses on both reproductive and non-reproductive systems. Nevertheless, our present observations could be helpful for the generation and application of CuNPs with desirable biological effects in veterinary and human medicine, and for the production of safe CuNPs-containing products.

Taken together, our observations confirm the direct, mainly stimulatory, impact of CuNPs on ovarian cells and their ability to affect their viability, proliferation, apoptosis and steroid hormones release. Furthermore, to the best of our knowledge, this represents the first demonstration that the nature of the CuNPs' action depends on their shape (spherical, triangular, hexagonal) and support (zeolite Y, TiO_2 or activated charcoal). Therefore, CuNPs with appropriate chemical modification could be potentially useful to control reproductive processes and to treat reproductive disorders.

List of abbreviations:

APVV: Slovak Research and Development Agency

Bax: BCL2 Associated X, Apoptosis Regulator

DMEM/F12: Dulbecco Modified Eagle's Medium + Ham's F12 medium, mixture 1:1

DTBB: 4,4′-di-*tert*-butylbiphenyl

CuNPs: copper nanoparticles

CuNPs/C: copper nanoparticles supported on charcoal

CuNPs/TiO_2: copper nanoparticles supported on titania

CuNPs/ZY: copper nanoparticles supported on zeolite Y

DHEA: dihydroepiandrosterone

ELISA: enzyme-linked immunosorbent assay

FITC: fluorescein isothiocyanate

GV: Generalitat Valenciana

ICP-OES: inductively coupled plasma-optical emission spectroscopy

ISO: Instituto de Síntesis Orgánica

MICIU - Spanish Ministerio de Ciencia, Innovación y Universidades

NFkB: nuclear factor kappa-light-chain-enhancer of activated B cells, transcription factor

PCNA: proliferation cell nuclear antigen

THF: tetrahydrofuran

VEGA: Slovak Grant Agency of the Ministry of Education, Science and Sport, and the Slovak Academy of Science

Acknowledgments:

These studies were supported by the Slovak Research and Development Agency (APVV; project no. APVV-15-0296), the Slovak Grant Agency of the Ministry of Education, Science and Sport, and the Slovak Academy of Science (VEGA; project no. VEGA 1/0392/17). This work was also generously supported by the Spanish Ministerio de Ciencia, Innovación y Universidades (MICIU; project no. CTQ2017-88171-P), the Generalitat Valenciana (GV; project no. AICO/2017/007), and the Instituto de Síntesis Orgánica (ISO). I.M.-G. thanks the Vicerrectorado de Investigación y Transferencia del Conocimiento of the Universidad de Alicante for a pre-doctoral grant (no. UAFPU2016-034).

DECLARATION OF INTEREST

The authors declare no conflicts of interest

REFERENCES

Abdulkin P, Moglie Y, Knappett BR, Jefferson DA; Yus M, Alonso F, Wheatley AEH. 2013. New routes to Cu(I)/Cu nanocatalysts for the multicomponent click synthesis of 1,2,3-triazoles. Nanoscale 5:342-350. doi: 10.1039/c2nr32570e.

Al-Bairuty GA, Shaw BJ, Handy RD, Henry TB. 2013. Histopathological effects of waterborne copper nanoparticles and copper sulphate on the organs of rainbow trout (*Oncorhynchus mykiss*). Aquat. Toxicol. 126:104-15. doi: 10.1016/j.aquatox.2012.10.005.

Alonso F., Yus M. 2008. New synthetic methodologies based on active transition metals. Pure Appl. Chem. 80:1005-1012. doi: 10.1351/pac200880051005.

Alonso F, Moglie Y, Radivoy G, Yus M. 2011. Click chemistry from organic halides, diazonium salts and anilines in water catalysed by copper nanoparticles on activated carbon. Org. Biomol. Chem. 9:6385-6395. doi: 10.1039/C1OB05735A.

Alonso F, Arroyo A, Martín-García I, Moglie Y. 2015. Cross-dehydrogenative coupling of tertiary amines and terminal alkynes catalyzed by copper nanoparticles on zeolite. Adv. Synth. Catal. 357: 3549-3561. doi: 10.1002/adsc.201500787.

Ameh T, Sayes CM. 2019. The potential exposure and hazards of copper nanoparticles: A review. Environ. Toxicol. Pharmacol. 71:103220. doi: 10.1016/j.etap.2019.103220.

Bhagyaraj SM, Oluwafemi OS, Kalarikkal N, Thomas S. 2018. Applications of Nanomaterials: Advances and Key Technologies, Woodhead Publishing, Cambridge, ISBN: 9780081019719.

Bourikas K, Kordulis C, Lycourghiotis A. 2014. Titanium dioxide (anatase and rutile): surface chemistry, liquid-solid interface chemistry, and scientific synthesis of supported catalysts. Chem. Rev. 114:9754. doi: 10.1021/cr300230q.

C A, Handral HK, Kelmani R C. 2018. A comparative in vivo scrutiny of biosynthesized copper and zinc oxide nanoparticles by intraperitoneal and intravenous administration routes in rats. Nanoscale Res. Lett. 13:93. doi: 10.1186/s11671-018-2497-2.

456 Carrol KJ, Reveles JU, Shultz MD, Khanna SN, Carpenter EE. 2011. Preparation of elemental
457 Cu and Ni nanoparticles by the polyol method: an experimental and theoretical approach. J.
458 Phys. Chem. C.115:2656-2664. doi: 10.1021/jp1104196.
459
460 Deka P, Borah BJ, Saikia H, Bharali P. 2019. Cu-based nanoparticles as emerging
461 environmental catalysts. Chem. Rec. 19:462-473. doi:10.1002/tcr.201800055.
462
463 Fevold HL, Hisaw FL, Greep R. 1936. Augmentation of the gonad-stimulating action of
464 pituitary extracts by inorganic substances, particularly copper salts. Am. J. Physiol. 117: 68-
465 74.
466
467 Fritsch J, Zingler P, Särchen V, Heck AL, Schütze S. 2017. Role of ubiquitination and
468 proteolysis in the regulation of pro- and anti-apoptotic TNF-R1 signaling. Biochim. Biophys.
469 Acta, Mol. Cell Res. 864(11 Pt B):2138-2146. doi:10.1016/j.bbamcr.2017.07.017.
470
471 Gawande MB, Goswami A, Felpin FX, Asefa T, Huang X, Silva R, Zou X, Zboril R, Varma
472 RS. 2016. Cu and Cu-based nanoparticles: synthesis and applications in catalysis. Chem. Rev.
473 116:3722-3811. doi: 10.1021/acs.chemrev.5b00482.
474
475 Gudipaty SA, Conner CM, Rosenblatt J, Montell DJ. 2018. Unconventional ways to live and
476 die: cell death and survival in development, homeostasis, and disease. Annu. Rev. Cell Dev.
477 Biol. 234:311-332. doi: 10.1146/annurev-cellbio-100616-060748.
478

Hedayati A, Hoseini SM, Hoseinifar SH. Response of plasma copper, ceruloplasmin, iron and ions in carp, Cyprinus carpio to waterborne copper ion and nanoparticle exposure. 2016. Comp. Biochem. Physiol., Part C: Toxicol. Pharmacol. 197:87–93. doi: 10.1016/j.cbpc.2015.09.007.

Hejazy M, Koohy MK, Pour ABM, Najafi D. 2018. Toxicity of manufactured copper nanoparticles – a review. Nanomed Res J 3: 1-9. doi: 10.22034/nmrj.2018.01.001.

Hoseini SM, Hedayati A, Mirghaed AT, Ghelichpur M. 2016. Toxic effects of copper sulfate and copper nanoparticles on minerals, enzymes, thyroid hormones and protein fractions of plasma and histopathology in common carp *Cyprinus carpio*. Exp. Toxicol. Pathol. 68:493–503. doi: 10.1016/j.etp.2016.08.002.

Hou J, Wang X, Hayat T, Wang X. 2017. Ecotoxicological effects and mechanism of CuO nanoparticles to individual organisms. Environ Pollut. 221:209-217. doi: 10.1016/j.envpol.2016.11.066.

Kumar CSSR, (Ed.) 2009. Metallic Nanomaterials, Wiley-VCH, Weinheim, ISBN: 9783527321513.

Liu Y, Liang J, Wang Q, He Y, Chen Y. 2016. Copper nanoclusters trigger muscle cell apoptosis and atrophy in vitro and in vivo. J. Appl. Toxicol. 36:454-463. doi: 10.1002/jat.3263.

503 Martín-García I, Alonso F. 2018. Synthesis of dihydroindoloisoquinolines through the
504 copper-catalyzed cross-dehydrogenative coupling of tetrahydroisoquinolines and nitroalkanes.
505 Chem. Eur. J. 24:18857-18862. doi: 10.1002/chem.201805137.
506
507 Minorics R, Zupko I. 2018. Steroidal anticancer agents: an overview of estradiol-related
508 compounds. Anticancer Agents Med Chem. 18:652-666. doi:
509 10.2174/1871520617666171114111721.
510
511 Mitrofanov A Y, Murashkina AV, Martín-García I, Alonso F, Beletskaya IP. 2017. Formation
512 of C-C, C-S and C-N bonds catalysed by supported copper nanoparticles. Catal. Sci. Technol.
513 7: 4401-4412. doi: 10.1039/C7CY01343D.
514
515 Noureen A, Jabeen F, Tabish TA, Zahoor MK, Ali M, Iqbal R, Yaqub S, Chaudhry AS. 2018.
516 Ameliorative effects of Moringa oleifera on copper nanoparticle induced toxicity in Cyprinus
517 carpio assessed by histology and oxidative stress markers. Nanotechnology 29:464003. doi:
518 10.1088/1361-6528/aade23.
519
520 Peña-Blanco A, García-Sáez AJ. 2018. Bax, Bak and beyond - mitochondrial performance in
521 apoptosis. FEBS J. 285:416-431. doi: 10.1111/febs.14186.
522
523 Pérez-Garijo A, Steller H. 2015. Spreading the word: non-autonomous effects of apoptosis
524 during development, regeneration and disease. Development. 142:3253-3262. doi:
525 10.1242/dev.127878.
526

527 Pohanka M. 2019. Copper and copper nanoparticles toxicity and their impact on basic
528 functions in the body. Bratisl. Lek Listy. 120:397-409. doi: 10.4149/BLL_2019_065.
529
530 Rathore K, Sharma K. 2018. Biological synthesis of copper nanoparticles and their
531 antimicrobial properties: a review. World J. Pharmaceut. Res. 7:11-26. doi:
532 10.4236/oalib.preprints.1200067.
533
534 Reddy LH, Arias JL, Nicolas J, Couvreur P. 2012. Magnetic nanoparticles: design and
535 characterization, toxicity and biocompatibility, pharmaceutical and biomedical applications.
536 Chem. Rev. 112:5818-5878. doi: 10.1021/cr300068p.
537
538 Roychoudhury S, Bulla J, Sirotkin AV, Kolesarova A. 2014. In vitro changes in porcine
539 ovarian granulosa cells induced by copper. J. Environ. Sci. Health A Tox. Hazard. Subst.
540 Environ. Eng. 49:625-633. doi: 10.1080/10934529.2014.865404.
541
542 Roychoudhury S, Nath S, Massanyi P, Stawarz R, Kacaniova M, Kolesarova A. 2016.
543 Copper-induced changes in reproductive functions: in vivo and in vitro effects. Physiol. Res.
544 65:11-22. ISSN: 0862-8408.
545
546 Sharma A, Boise LH, Shanmugam M. 2019. Cancer metabolism and the evasion of apoptotic
547 cell death. Cancers (Basel). 11: pii: E1144. doi: 10.3390/cancers11081144.
548

549 Shaw BJ, Al-Bairuty G, Handy RD. Effects of waterborne copper nanoparticles and copper
550 sulphate on rainbow trout, (*Oncorhynchus mykiss*): physiology and accumulation. 2012.
551 Aquat. Toxicol. 116-117:90–101. doi: 10.1016/j.aquatox.2012.02.032.

552

553 Sirotkin AV. 2014. Regulators of Ovarian Functions. Nova Publishers Inc., New York, p.194.
554 ISBN: 978-1-61668-040-4.

555

556 Sirotkin AV, Alexa R, Dekanova P, Kadasi A, Stochmalova A, Grossmann R, Alwasel SH,
557 Harrath AH. 2015. The mTOR system can affect basic ovarian cell functions and mediate the
558 effect of ovarian hormonal regulators. Int. J. Pharmacol. 11:570–578. doi:
559 10.3923/ijp.2015.570.578

560

561 Stark WJ, Stoessel PR, Wohlleben W, Hafner A. 2015. Industrial applications of
562 nanoparticles. Chem. Soc. Rev. 44:5793-5805. doi: 10.1039/c4cs00362d.

563

564 Strober W. 2001. Trypan blue exclusion test of cell viability. Curr. Protoc. Immunol.
565 Appendix 3B. doi: 10.1002/0471142735.ima03bs21.

566

567 Sutunkova MP, Privalova LI, Minigalieva IA, Gurvich VB, Panov VG, Katsnelson BA. 2018.
568 The most important inferences from the Ekaterinburg nanotoxicology team's animal
569 experiments assessing adverse health effects of metallic and metal oxide nanoparticles.
570 Toxicol. Rep. 5:363-376. doi:10.1016/j.toxrep.2018.03.008.

571

572 Verma N, Kumar N. 2019. Synthesis and biomedical applications of copper oxide
573 nanoparticles: an expanding horizon. ACS Biomater. Sci. Engin. 5:1170-1188. doi:
574 10.1021/acsbiomaterials.8b01092

575

576 Wang SC. 2014. PCNA: a silent housekeeper or a potential therapeutic target? Trends
577 Pharmacol Sci 35:178–186. doi: 10.1016/j.tips.2014.02.004.

578

579 Yang J, Hu S, Rao M, Hu L, Lei H, Wu Y, Wang Y, Ke D, Xia W, Zhu CH. 2017. Copper
580 nanoparticle-induced ovarian injury, follicular atresia, apoptosis, and gene expression
581 alterations in female rats. Int. J. Nanomedicine. 12:5959-5971. doi: 10.2147/IJN.S139215.

582

583 Zhang CH, Wang Y, Sun QQ, Xia LL, Hu JJ, Cheng K, Wang X, Fu XX, Gu H. 2018.
584 Copper nanoparticles show obvious in vitro and in vivo reproductive toxicity via erk mediated
585 signaling pathway in female mice. Int. J. Biol. Sci. 14:1834-1844. doi: 10.7150/ijbs.27640.

586

587 Zhou M, Tian M, Li C. 2016. Copper-based nanomaterials for cancer imaging and therapy.
588 Bioconjugate Chem. 27:1188-1199. doi: 10.1021/acs.bioconjchem.6b00156.

589

590

591

592

593

594

FIGURES AND LEGENDS

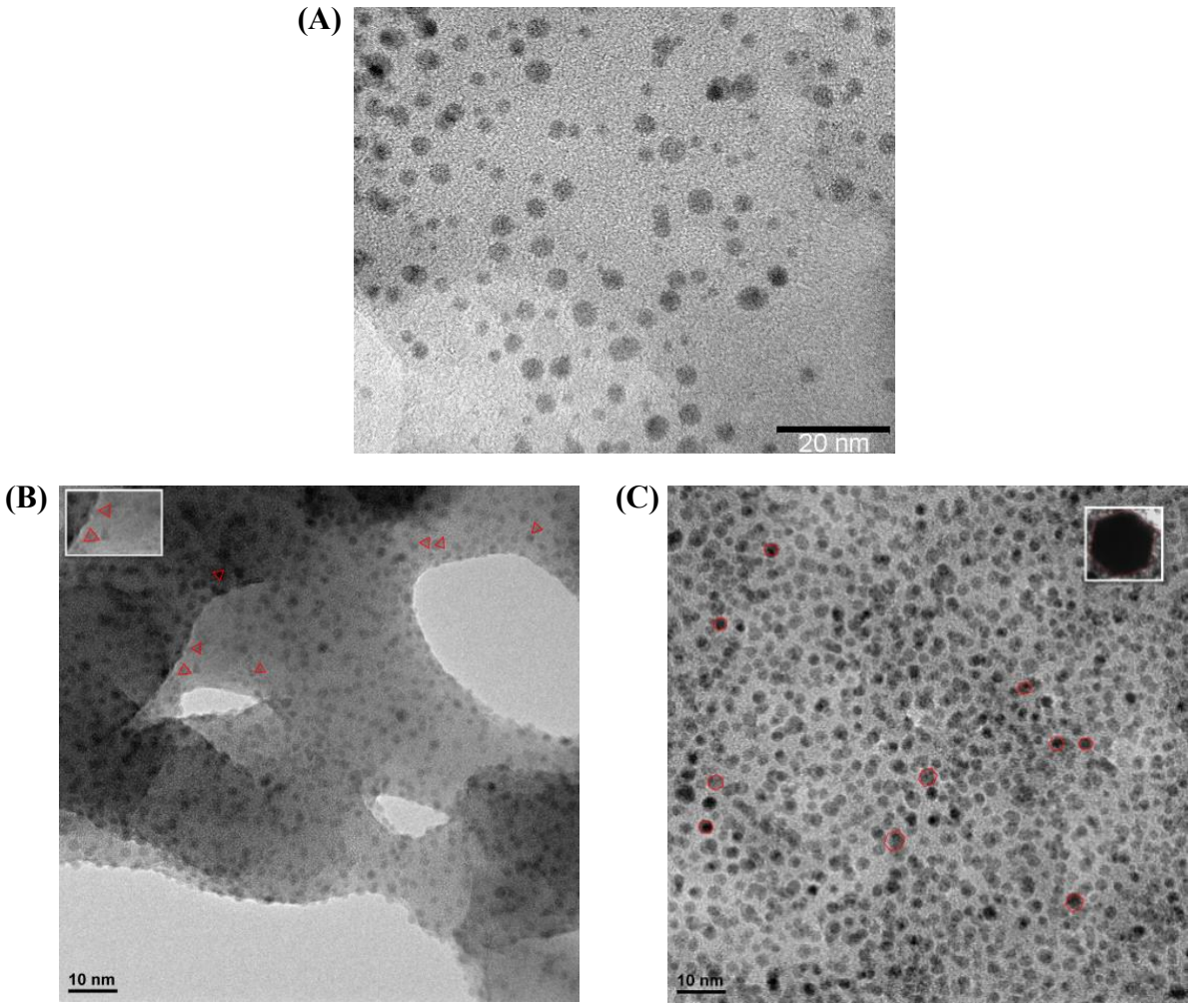

Figure 1. Transmission electron microscopy micrographs of spherical (**A**), triangular (**B**) and hexagonal (**C**) CuNPs.

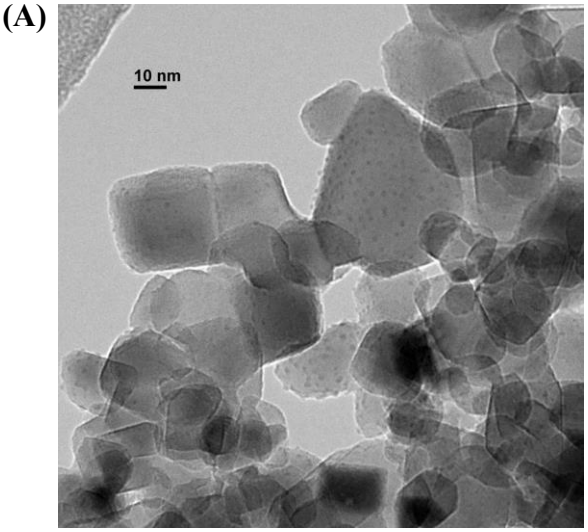

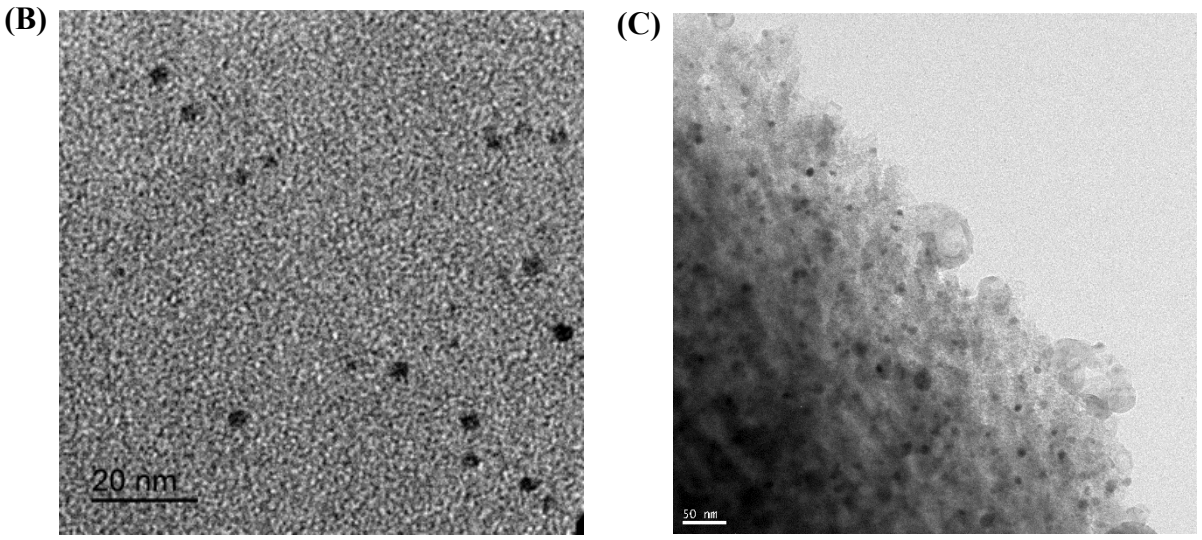

Figure 2. Transmission electron microscopy micrographs of supported CuNPs/TiO_2 (**A**), CuNPs/ZY (**B**) and CuNPs/C (**C**).

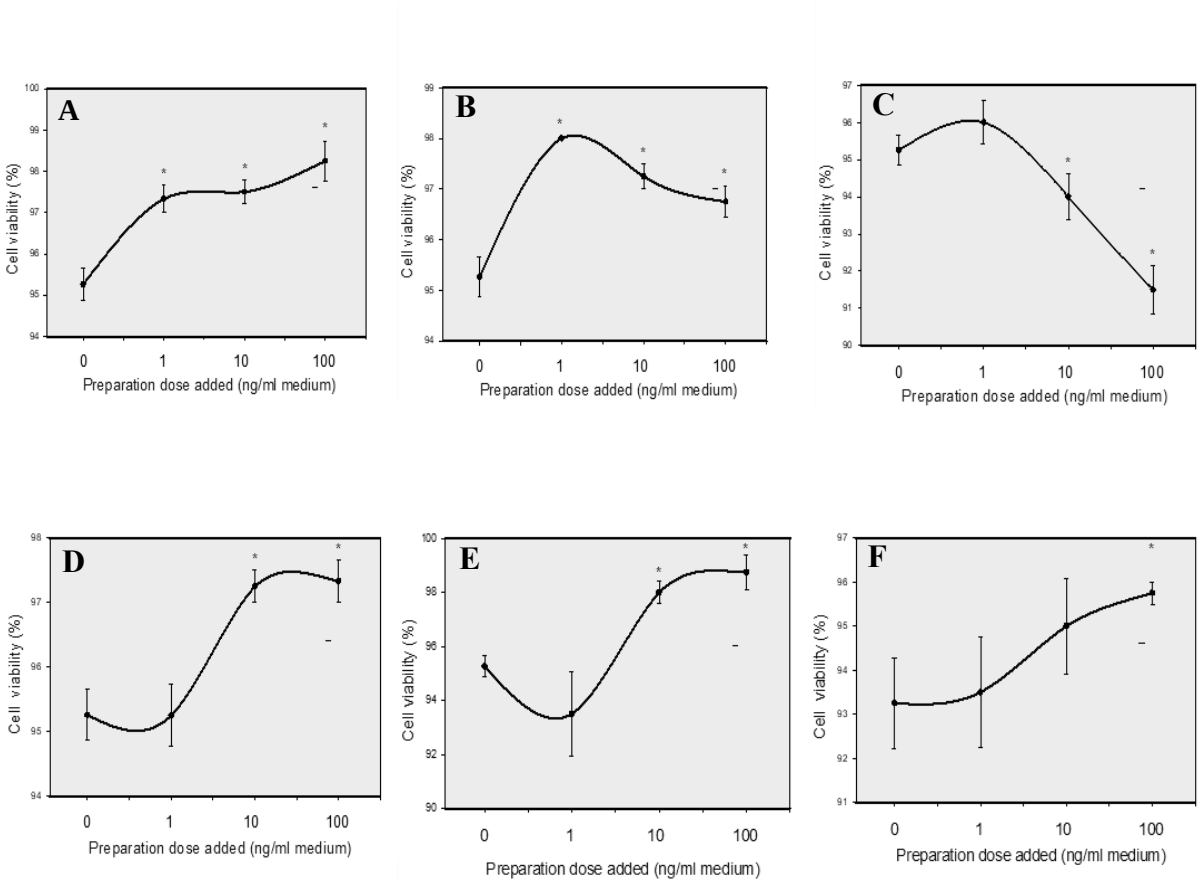

Figure 3. Comparison of the effect of spherical (**A**), triangular (**B**), hexagonal (**C**) CuNPs, and spherical CuNPs/TiO_2 (**D**), CuNPs/ZY (**E**) and CuNPs/C (**F**), added at the doses of 0, 1, 10 or 100 ng/mL medium, on viability (measured by the Trypan blue extrusion test) of cultured porcine ovarian granulosa cells. Each experiment was repeated three times using different animals. Each experimental group was represented by four chamber-slide wells (n = 12). Values are presented as the mean ± S.D.; the asterisk indicates the effect of treatment – significant ($P < 0.05$) differences between cells treated versus untreated (dose 0 ng/mL) with nanoparticles.

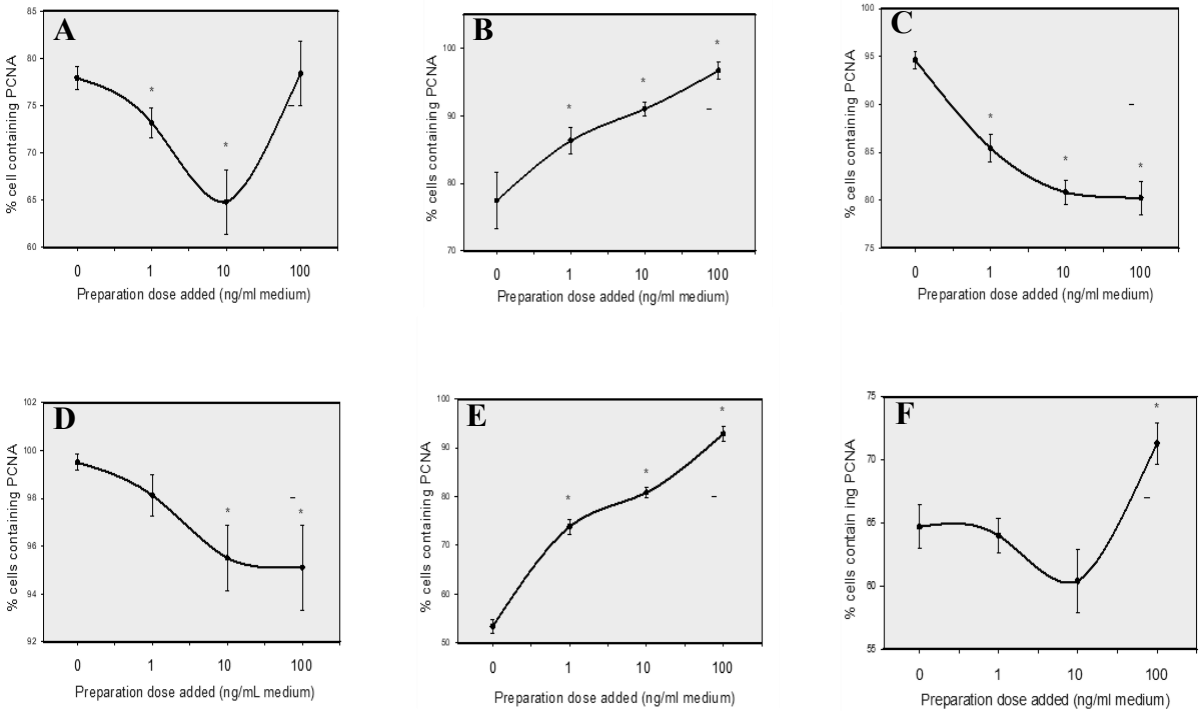

614

615 **Figure 4.** Comparison of the effect of spherical (**A**), triangular (**B**), hexagonal (**C**) CuNPs,
616 and spherical CuNPs/TiO_2 (**D**), CuNPs/ZY (**E**) and CuNPs/C (**F**), added at the doses of 0, 1,
617 10 or 100 ng/mL medium, on proliferation (accumulation of PCNA measured by quantitative
618 immunocytochemistry) of cultured porcine ovarian granulosa cells. Each experiment was
619 repeated three times using different animals. Each experimental group was represented by
620 four chamber-slide wells (n = 12). Values are presented as the mean ± S.D.; the asterisk
621 indicates the effect of treatment – significant ($P < 0.05$) differences between cells treated
622 versus untreated (dose 0 ng/mL) with nanoparticles.

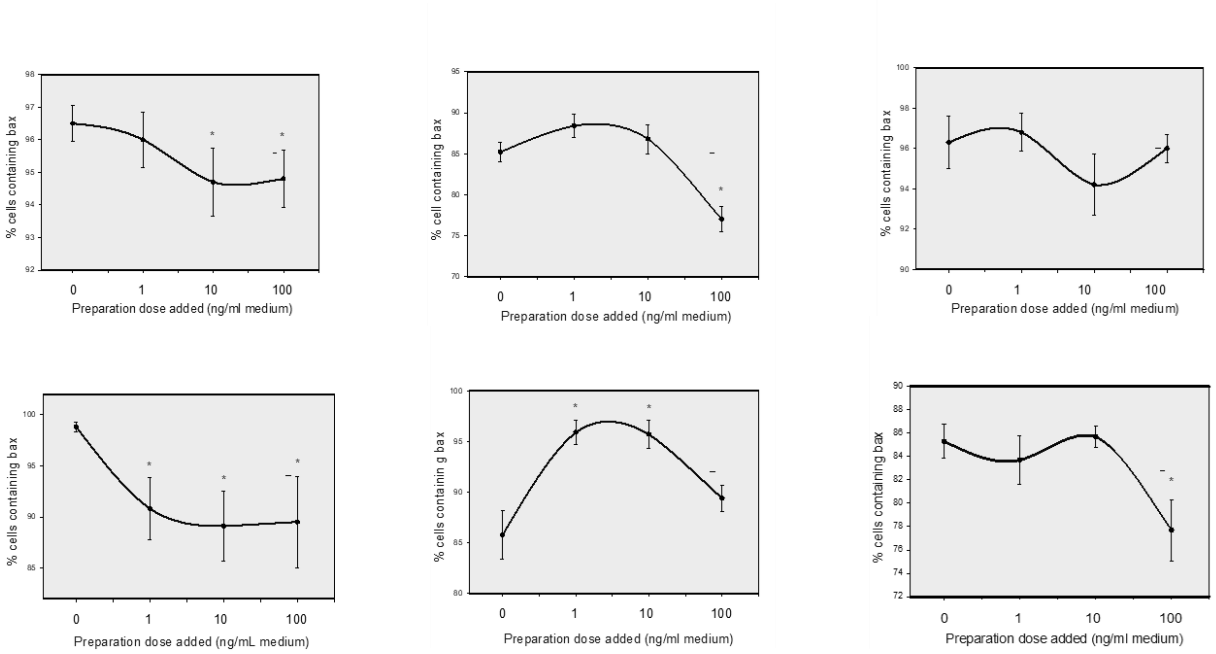

623

624 **Figure 5.** Comparison of the effect of spherical (**A**), triangular (**B**), hexagonal (**C**) CuNPs,
625 and spherical CuNPs/TiO_2 (**D**), CuNPs/ZY (**E**) and CuNPs/C (**F**), added at the doses of 0, 1,
626 10 or 100 ng/mL medium on apoptosis (accumulation of bax measured by quantitative
627 immunocytochemistry) by cultured porcine ovarian granulosa cells. Each experiment was
628 repeated three times using different animals. Each experimental group was represented by
629 four chamber-slide wells (n = 12). Values are presented as the mean ± S.D.; the asterisk
630 indicates the effect of treatment – significant ($P < 0.05$) differences between cells treated
631 versus untreated (dose 0 ng/mL) with nanoparticles.

632

633

634

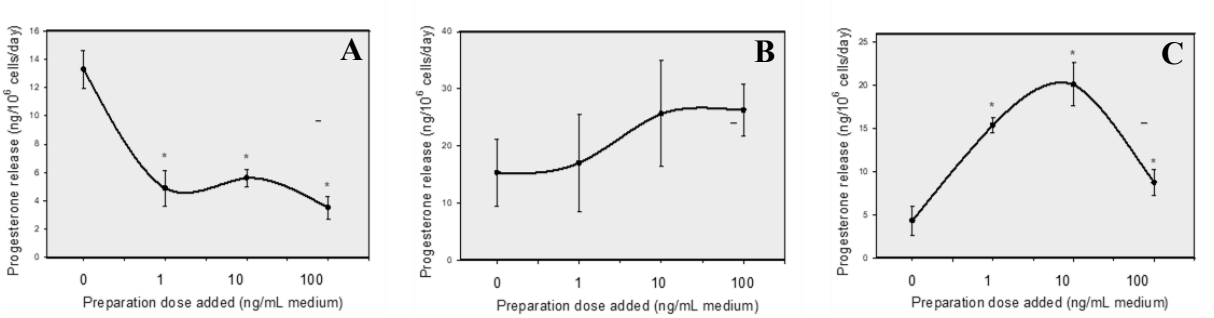

635

636 **Figure 6.** Comparison of the effect of spherical CuNPs/TiO_2 (**A**), CuNPs/ZY (**B**) and
637 CuNPs/C (**C**), added at the doses of 0, 1, 10 or 100 ng/mL medium on the release of
638 progesterone (measured by ELISA) by cultured porcine ovarian granulosa cells. Each
639 experiment was repeated three times using different animals. Each experimental group was
640 represented by four chamber-slide wells (n = 12). Values are presented as the mean ± S.D.;
641 the asterisk indicates the effect of treatment – significant ($P < 0.05$) differences between cells
642 treated versus untreated (dose 0 ng/mL) with nanoparticles.

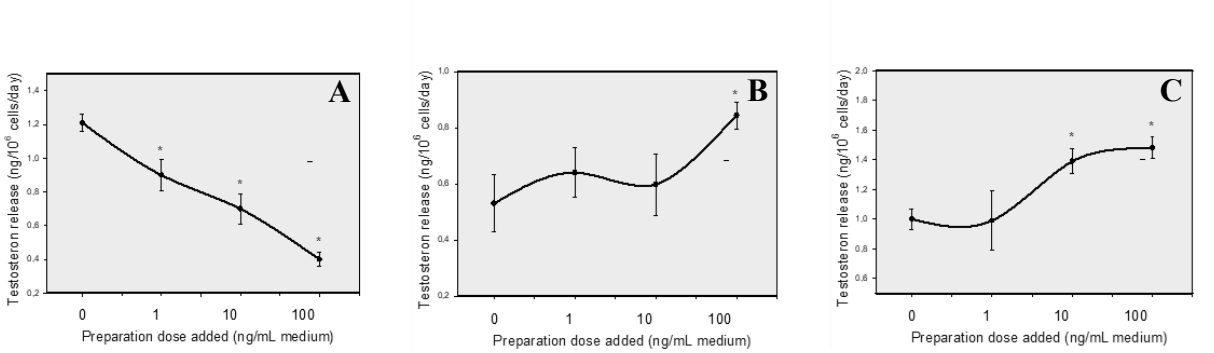

643

644 **Figure 7.** Comparison of the effect of spherical CuNPs/TiO_2 (**A**), CuNPs/ZY (**B**) and
645 CuNPs/C (**C**), added at the doses of 0, 1, 10 or 100 ng/mL medium on the release of
646 testosterone (measured by ELISA) by cultured porcine ovarian granulosa cells. Each
647 experiment was repeated three times using different animals. Each experimental group was
648 represented by four chamber-slide wells (n = 12). Values are presented as the mean ± S.D.;
649 the asterisk indicates the effect of treatment – significant ($P < 0.05$) differences between cells
650 treated versus untreated (dose 0 ng/mL) with nanoparticles.

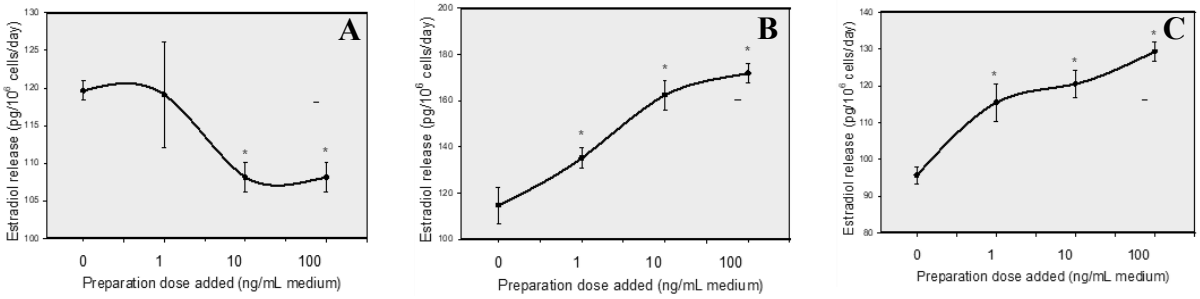

Figure 8. Comparison of the effect of spherical CuNPs/TiO_2 (**A**), CuNPs/ZY (**B**) and CuNPs/C (**C**), added at the doses of 0, 1, 10 or 100 ng/mL medium on the release of 17*β*-estradiol (measured by ELISA) by cultured porcine ovarian granulosa cells. Each experiment was repeated three times using different animals. Each experimental group was represented by four chamber-slide wells (n = 12). Values are presented as the mean ± S.D.; the asterisk indicates the effect of treatment – significant ($P < 0.05$) differences between cells treated versus untreated (dose 0 ng/mL) with nanoparticles.